Report

Decoding Biological Elegance: Unveiling the Intricacies of Gene ME480 through the Lens of Deformability Cytometry

Omar Saubry[1], Mehmet Furkan Doğan[2], Matthieu Scharffe[2], Charles De Fournas[2], and Cemal Kaan Köse[2]

[1]SV, EPFL
[2]GM, EPFL

ABSTRACT Utilizing flow cytometry, we subjected modified cells to shear stress to elucidate the influence of the ME480 gene on cellular mechanical properties. Our study highlights both the utility and constraints of flow cytometry in distinguishing cells, particularly in the context of pharmacological applications.

INTRODUCTION

Deformability cytometry is an innovative method employed for the structural analysis of cells. By guiding cells through a confined microfluidic channel, a specific shear stress is applied to them.

Cellular structural integrity relies on two key mechanisms: the cytoskeleton and the cell membrane. Deformability cytometry serves as a means to distinguish cells with varying cytoskeletal or membrane properties. Our objective was to utilize this method to investigate the potential influence of the ME480 gene on cellular mechanics.

To address this inquiry, we conducted two experiments. In the first, we suppressed the expression of the gene and selected different samples. Subsequently, we allowed the gene to express over varying durations before commencing deformability cytometry on each sample. This approach enabled us to assess the correlation between gene expression and its impact on cell mechanics.

In the second experiment, we inhibited the gene in one set of cells while activating it in another. By comparing these two sets, we aimed to amplify the contrast in gene expression and, if any impact existed, magnify its effects. This experimental design allowed for a more pronounced evaluation of the gene's influence on cellular mechanics.

RESULTS

Different time for endogenously expression of ME480

Through the application of the sample preparation method, we conducted deformability cytometry flow experiments on various cell samples, calculating deformation relative to cell size.

In the initial analysis depicted in Figure 6, the scatter plots for different samples appear superimposable, making it challenging to draw conclusions regarding any differences associated with the expression of the ME480 gene. To gain a more nuanced perspective, we computed the mean values and the standard deviations of deformation and cell size for each run. Subsequently, in Figure 7, we performed cross-validation, affirming our initial analysis. We also performed statistical studies on other parameters in Figure 2, 3, 4, 5. The results support the conclusion that the expression of the ME480 gene did not enhance the mechanical properties of our cells. This lack of differentiation may be attributed to insufficient time for the gene to express itself, given that our longest expression time was 48 minutes.

To validate our findings that the ME480 gene does not influence the mechanical properties of the cell, we conducted a second experiment. In this trial, we utilized the cells modified as outlined in the latter part of the sample preparation.

Cell B, expressing the ME480 gene continuously for six consecutive days, provided a robust test to ascertain any potential impact on the mechanical structure of the cell. As illustrated in Figures 8, 9, the results mirrored those of our initial experiment, indicating no discernible difference between the two cell types.

Therefore, we can confidently affirm that the ME480 gene does not exert an impact on the mechanical properties of the cell.

DISCUSSION AND CONCLUSION

In our study, we demonstrate that analyzing cell structure to discern gene expression, specifically the ME480 gene, is not always feasible, as it does not always influence the mechanical properties of the cell. The cytometry flow method is constrained in its applicability and specificity and cannot be employed for a total comprehensive cell analysis in pharmacological tests. Other tests are required to detect potential impacts from different genes.

Despite these limitations, the Real-Time Deformability Cytometry (RT-DC) method remains highly valuable in various scenarios. It provides a mean to analyze a large number of cells in a label free method as demonstrated in the study by (1), and could be combined with clustering machine learning methods, to allows for the differentiation of cells in distinct phases. Additionally, it can be employed to monitor the effects of certain drug administrations if they impact the mechanical properties of cell.

MATERIALS AND METHODS

Microfluidic experiments

Sample preparation: First Experience

To generate cells with altered expression of the ME480 gene, we employed a modified cell line known as CellA ShME480. This cell line has been engineered to incorporate a gene that, upon activation with doxycycline, silences the ME480 gene. Culturing of these cells spanned six days with continuous exposure to doxycycline, resulting in the development of cells devoid of the ME480 gene.

Subsequently, we allowed these modified cells to remain outside the influence of doxycycline, introducing variable time intervals to induce diverse expression patterns of ME480.

Run	Time since the cell are outside doxycycline [min]
1	00:15
2	00:19
3	00:24
4	00:29
5	00:35
6	00:39
7	00:43
8	00:48

Table 1: Time since detachment for each run

Sample preparation: Second Experience

In this sample preparation we used four different cell:

Cell Type	Reaction to doxycycline
cellA ShME480	Silence gene ME480
CellA GFP	Silence gene ME480, produce GFP
CellB ME480	Express gene ME480
CellB GFP	Express gene ME480, produce GFP

Table 2: Modified cell use for our different sample

We cultured these cells for a duration of six days in the presence of doxycycline. Subsequently, we harvested them from their midpoints and conducted cytometric flow experiments on the cells 15 minutes after their removal.

Flow Cytometry Parameters

In our cytometry experiment, we implemented the following parameter

- Cell sample flow rate: $4\,\mu L/\text{min}$
- Sheath flow rate: $12\,\mu L/\text{min}$
- Channel dimensions (length × width × depth): $300 \times 30 \times 30\,\mu m$

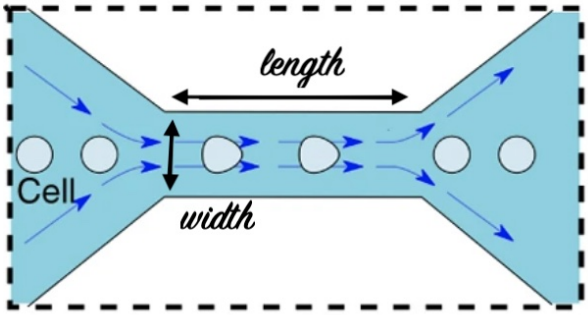

Figure 1: Schematic of microfluidic pathway for cytometry deformation

Image acquisition parameters

- **Camera :** Phantom VE 640 L
- **Image Type :** Phase contrast
- **Exposure time :** 1 µm
- **Frame Rate :** 10 000 fps
- **Number of frames per movie :** 356,953
- **Pixel size :** 10x10 µm
- **Magnification :** 30x
- **Image dimensions :** 256x128 pixels

Image processing

Compression

Our program uses a frame selection strategy based on Mean Squared Error (MSE). The process begins by loading the video using the *PIMS* library and initializing the reference frame as the first frame of the video. The goal is to identify and retain the relevant frames for deformability cytometry analysis, discarding redundant or empty frames. The script iterates through the video frames, comparing each frame's MSE with the reference frame. A threshold is set, and frames with an MSE higher than this threshold are considered relevant and stored in a list. This criterion is grounded in the assumption that

frames with substantial differences from the initial frame are more likely to contain cells and thus deformability information. Then, a new video is generated using the *FFmpegWriter* from the *skvideo.io* module. The resulting video exhibits a significant reduction in size.

Segmentation

For segmentation of the cells, we have mainly used two different methods. The first method was to use conventional image processing tools with Open CV python library (2). Since the brightness of the cells are not significantly different from the brightness of the background, it is not possible to use a simple threshold method to detect the shape of the cell. Because of that, we have used Canny edge detection algorithm to detect the borders of the cells. This method worked well for some of the cells but the parameters must be calibrated for different shape and sizes of cells to get a reliable results. On the other hand the advantage of this method is the computational simplicity.

The other method we tried to use a neural network model trained to detect cytoplasm of cells. We have used a python library that is designed to segment cells from microscopy images (3). Cellpose has two models for detecting the cytoplasm and nucleus of cells trained by using deep reinforcement learning on large data sets of microscopy images. In our case we have used the cytoplasm model since our aim is to segment the cells as a whole. The one disadvantage of this method is computational complexity. With the computational power that we have, it took around 1 second to segment a frame.

After careful consideration, we decided to use the segmentation results obtained using Cellpose, since it can produce more reliable results than using the Canny edge detection algorithm, even though Cellpose takes more time to compute the segmentation.

While we have not spent a lot of time making the segmentation more reliable by using the Canny algorithm, doing so would significantly reduce the computation time. Our recommendation for future researchers processing deformability cytometry data is to develop a segmentation algorithm that is as simple as possible.

Data analysis and statistical methods

From the wide range of statistical data given by image processing, we only kept a list of parameters that we thought relevant to characterize the cells' deformation:

- Area
- Perimeter
- Height
- Width
- Aspect Ratio

To compare the different runs, we computed the mean value and the standard deviation of each of the parameters. It allowed us to plot them as a bar chart with a confidence interval. There is also a second bar chart which corresponds to the relative difference of the run that gives the lowest value with the other runs.

To represent the cells on the graph, we assumed that their shape was an ellipse. Knowing the average height and width We could then display the ellipse of each run. We also aimed at computing a confidence interval for the ellipses with the standard deviation. However, we only show the result in the supplementary material as it is difficult to interpret due to the spreading of the data.

Poisson's ratio

We computed poisson's ratio (ν) to quantify the deformability of the cells. We made the assumption that the cells are circle before entering the pipe and that the total area is conserved. From the second assumption it is possible to derive, $R_{cell} = \frac{1}{2}\sqrt{Height \cdot Width}$. And finally :

$$\nu = \frac{2R_{cell} - Width}{Height - 2R_{cell}} \tag{1}$$

Deformation

After obtaining the cytometry deformability values, a crucial metric for evaluation is deformation (1), often expressed by the indicator:

$$D = 1 - 2 \cdot \frac{\sqrt{\pi \cdot Area}}{Perimeter}$$

This indicator provides insights into the strength of both the cytoskeleton and the cell membrane.

Porosity

Another important parameter we used for quantifying the deformation of the cells is porosity. Porosity is defined as the convex hull area divided by the measured area. It can also be defined as the reciprocal of solidity. It is greater than 1 for every non convex set. We have used porosity to filter the non-cellular particles. Particles with porosity greater than 1.05 are excluded from our analysis.

Inertia ratio

Inertia ratio is the ratio of the second moments of area along x and y axis. It is another parameter that can be used for measuring the deformation of the cells.

$$\text{inertia ratio} = \frac{I_y}{I_x} = \frac{\int_{cell} x^2 dxdy}{\int_{cell} y^2 dxdy} \tag{2}$$

Figures and Tables

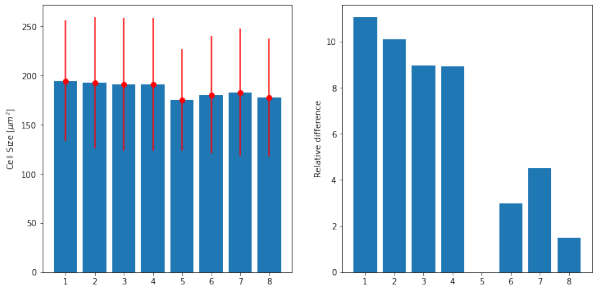

Figure 2: Bar chart of the evolution of the area of the cells of the different runs of part B

The other parameters that can be found in the *supplementary material*, as Figures 10, 11, 12, 13, display a similar trend for the relative difference (in %). The maximum relative difference that we can get is close to 15% for all the statistical parameters. It is a value to mitigate as the data are highly spread.

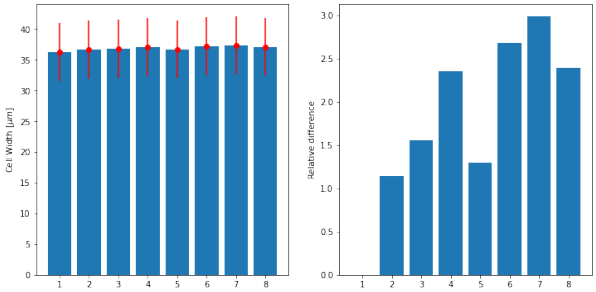

Figure 3: Bar chart of the evolution of the width of the cells of the different runs of part B

For this parameter, the relative difference displays a different trend that for the other parameters. Nonetheless, the values are very low.

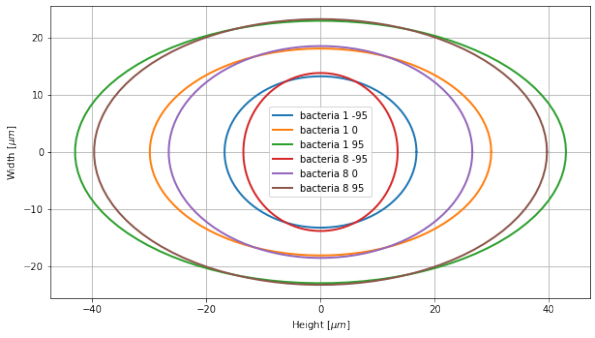

Figure 4: Mean ellipses with the associated ellipses of the min and max of the 95% confidence interval of the first and last run of part B.

Just as the two previous figures have shown, it is difficult to state that the gene ME480 has an impact on the mechanical properties of the cell due to the spread data.

The *Supplementary material* shows the mean ellipses of all the runs (Figure 14), the mean ellipses of the first and last run (Figure 15) and the mean ellipses of the largest and smallest run (Figure 16) which corresponds to the first and fifth run.

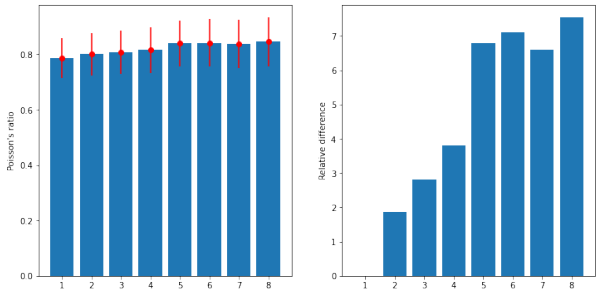

Figure 5: Bar chart of the evolution of the Poisson's ratio of the cells of the different runs of part B.

One of the assumption made to compute poisson's ratio may be wrong as the computed values are higher than 0.5. It is most likely to be the conservation of the area. However, it still gives an interesting glimpse of the effect of the gene.

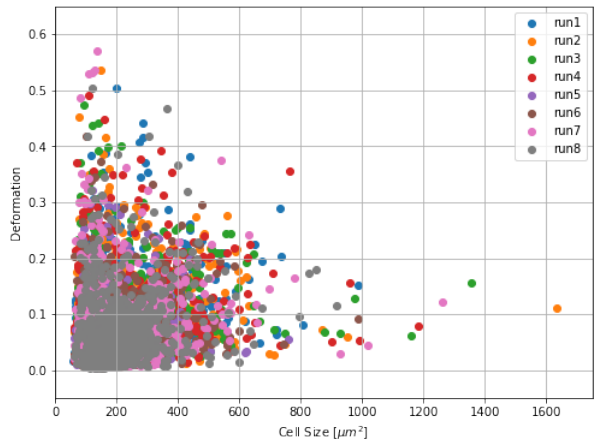

Figure 6: Scatter plot illustrating the relationship between deformation and cell size across various samples of part B

The deformation value points of all the runs are similar. It is difficult to make an opinion out of it. So, we computed the mean values with a confidence interval of one standard deviation to better understand.

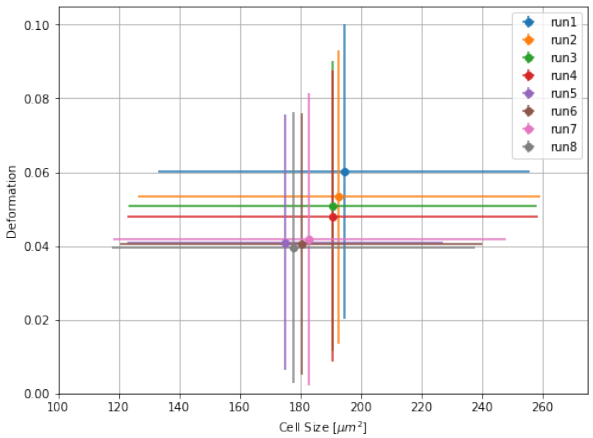

Figure 7: Scatter plot illustrating the relationship between mean deformation and mean cell size across various samples of part B

The observed decrease does not appear to be statistically significant, as even the farthest data points fall within one standard deviation.

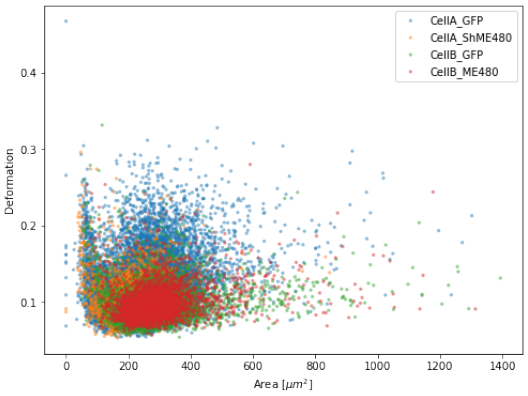

Figure 8: Deformation versus cell area scatter plot of cells CellA GFP, CellA ShME480, CellB GFP and CellB ME480 labeled with different colors

This plot is similar to Figure 6. It is here to compare the different expressions of the gene.

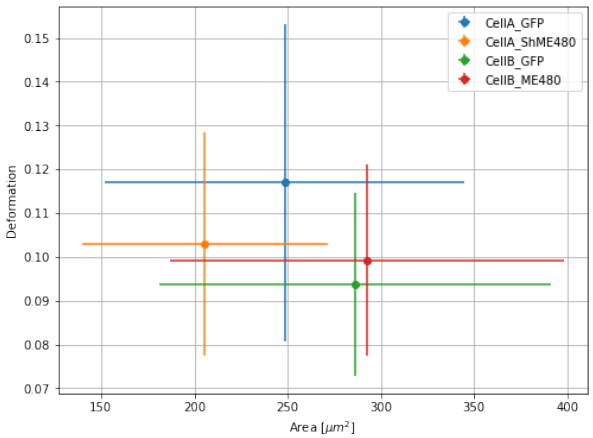

Figure 9: Deformation versus cell area mean values plot of cells CellA GFP, CellA ShME480, CellB GFP and CellB ME480 labeled with different colors

As before, the statistical variations don't seem to appear significant. The *Supplementary material* show other parameters that have been under study for the different cell types in Figures 17, 18, 19, 20.

CODE AVAILABILITY

Code for segmentation and analysis of microscopy images is published on github.com/mehmetfurkandogan/deformability-cytometry/.

REFERENCES

1. Otto, O., P. Rosendahl, A. Mietke, S. Golfier, C. Herold, D. Klaue, S. Girardo, S. Pagliara, A. Ekpenyong, A. Jacobi, et al., 2015. Real-time deformability cytometry: on-the-fly cell mechanical phenotyping. *Nature methods* 12:199–202.

2. Bradski, G., 2000. The OpenCV Library. *Dr. Dobb's Journal of Software Tools* .

3. Stringer, C., T. Wang, M. Michaelos, and M. Pachitariu, 2021. Cellpose: a generalist algorithm for cellular segmentation. *Nature methods* 18:100–106.

SUPPLEMENTARY MATERIAL

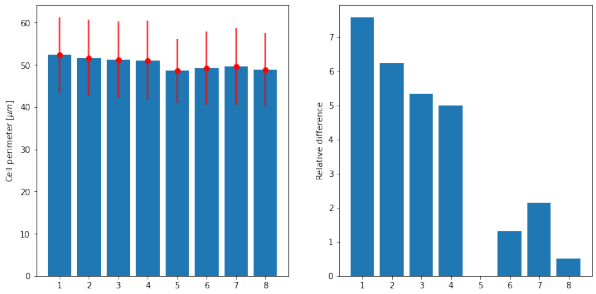

Figure 10: Bar chart of the evolution of the Perimeter of the cells of the different runs of part B

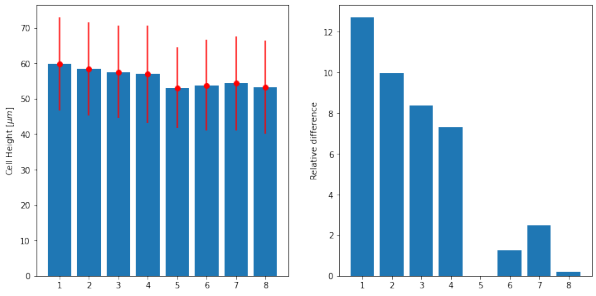

Figure 11: Bar chart of the evolution of the Height of the cells of the different runs of part B

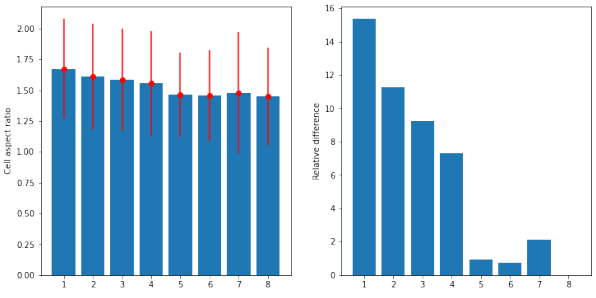

Figure 12: Bar chart of the evolution of the Aspect Ratio of the cells of the different runs of part B

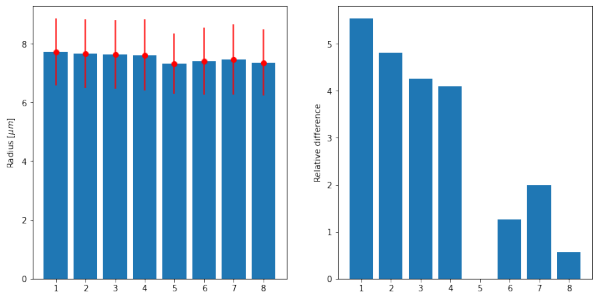

Figure 13: Bar chart of the evolution of the Radius of the cells of the different runs of part B

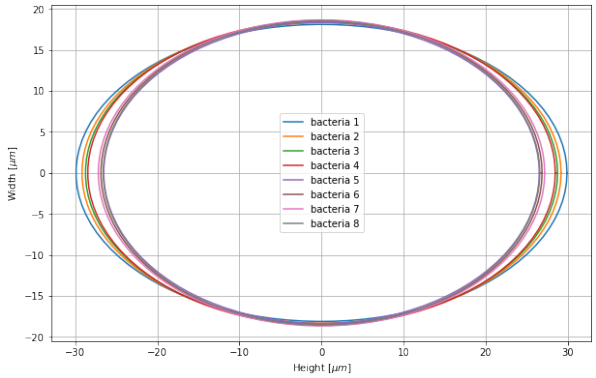

Figure 14: Mean ellipses of all the runs of part B

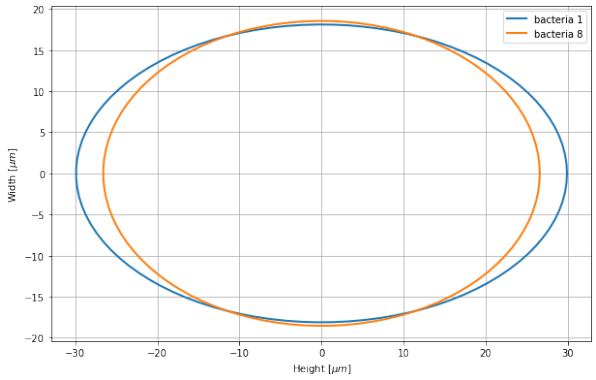

Figure 15: Mean Ellipses of the firt and last run of part B

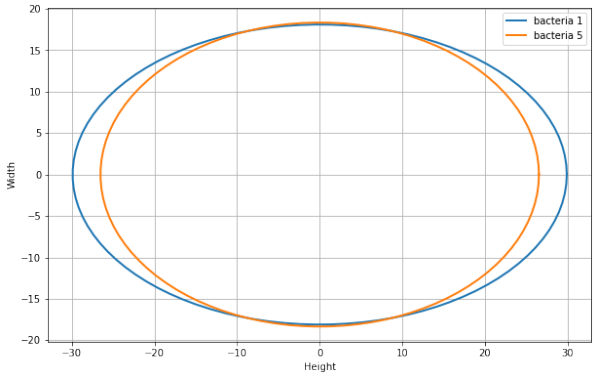

Figure 16: Mean ellipses of the largest and smallest run of part B

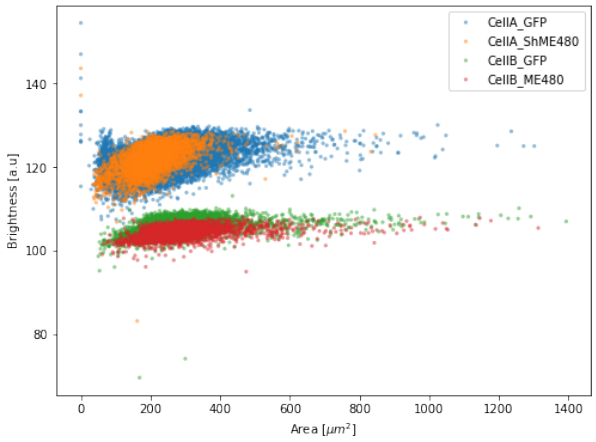

Figure 17: Brightness versus cell area scatter plot of cells CellA GFP, CellA ShME480, CellB GFP and CellB ME480 labeled with different colors

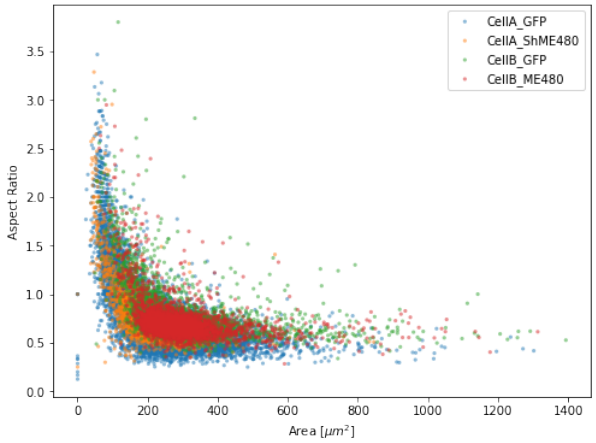

Figure 18: Aspect ratio versus cell area scatter plot of cells CellA GFP, CellA ShME480, CellB GFP and CellB ME480 labeled with different colors

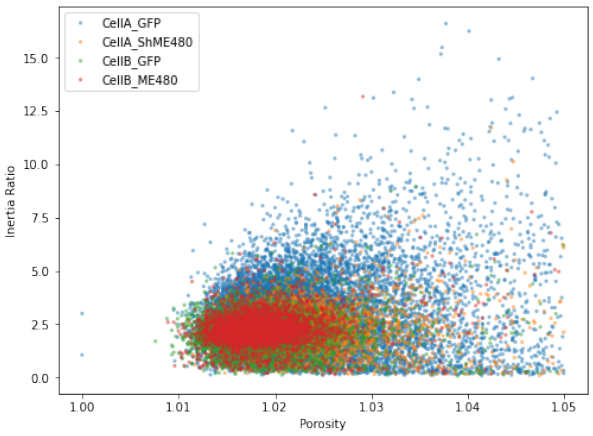

Figure 19: Inertia ratio versus porosity scatter plot of cells CellA GFP, CellA ShME480, CellB GFP and CellB ME480 labeled with different colors

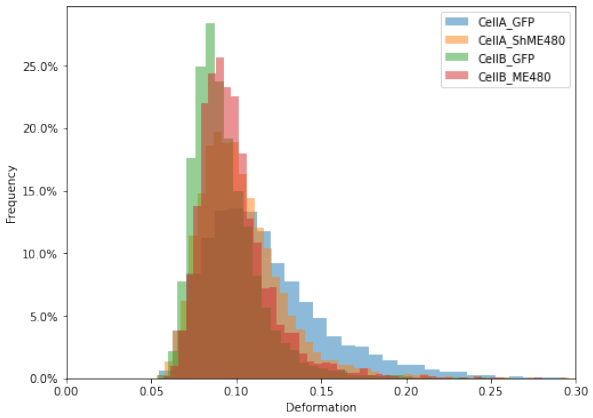

Figure 20: Histogram of the deformation of cells CellA GFP, CellA ShME480, CellB GFP and CellB ME480 labeled with different colors